The Anaphase Promoting Complex Regulates Yeast Lifespan and rDNA Stability by Targeting Fob1 for Degradation

Johannes Menzel,* Mackenzie E. Malo,* Cynthia Chan,* Martin Prusinkiewicz,* Terra G. Arnason,† and Troy A. A. Harkness*,1

*Department of Anatomy and Cell Biology, and †Department of Medicine, College of Medicine, University of Saskatchewan, Saskatoon, Saskatchewan, S7N 5E5, Canada

ABSTRACT Genomic stability, stress response, and nutrient signaling all play critical, evolutionarily conserved roles in lifespan determination. However, the molecular mechanisms coordinating these processes with longevity remain unresolved. Here we investigate the involvement of the yeast anaphase promoting complex (APC) in longevity. The APC governs passage through M and G1 via ubiquitin-dependent targeting of substrate proteins and is associated with cancer and premature aging when defective. Our two-hybrid screen utilizing Apc5 as bait recovered the lifespan determinant Fob1 as prey. Fob1 is unstable specifically in G1, cycles throughout the cell cycle in a manner similar to Clb2 (an APC target), and is stabilized in APC (*apc5^{CA}*) and proteasome (*rpn10*Δ) mutants. Deletion of *FOB1* increased replicative lifespan (RLS) in wild type (WT), *apc5^{CA}*, and *apc10*Δ cells, and suppressed *apc5^{CA}* cell cycle progression and rDNA recombination defects. Alternatively, increased *FOB1* expression decreased RLS in WT cells, but did not reduce the already short *apc5^{CA}* RLS, suggesting an epistatic interaction between *apc5^{CA}* and *fob1*Δ. Mutation to a putative L-Box (Fob1^{E420V}), a Destruction Box-like motif, abolished Fob1 modifications, stabilized the protein, and increased rDNA recombination. Our work provides a mechanistic role played by the APC to promote replicative longevity and genomic stability in yeast.

THE anaphase promoting complex (APC) is a ubiquitin-protein ligase (E3) that is conserved from yeast to humans (Harper *et al.* 2002; Passmore 2004; Barford 2011; McLean *et al.* 2011). The APC in yeast is composed of 13 core subunits that interact with the cell-cycle-specific substrate-binding adaptors Cdc20 or Cdh1. Eight of the 13 yeast APC subunits are essential, with conditional alleles resulting in cell cycle arrest at the anaphase/metaphase junction (Zachariae and Nasmyth 1999). The APC is required for progression through mitosis and maintenance of G1, functions carried out through the targeted degradation of protein substrates that block sister chromatid separation, and exit from mitosis. The list of APC substrates in yeast continues to grow (Qiao *et al.* 2010; Ostapenko *et al.* 2012; Ferguson *et al.* 2013).

doi: 10.1534/genetics.113.158949
Manuscript received October 24, 2013; accepted for publication December 9, 2013; published Early Online December 20, 2013.
[1]Corresponding author: Department of Anatomy and Cell Biology, University of Saskatchewan, B313 Health Sciences Bldg., 107 Wiggins Rd., Saskatoon, SK S7N 5E5, Canada. E-mail: troy.harkness@usask.ca

The list of cellular functions that involve the APC also continues to grow. These functions include maintenance of genomic stability and control of chromatin metabolism. Several reports demonstrate that APC mutants result in loss of chromosomes and plasmids at accelerated rates (Hartwell and Smith 1985; Palmer *et al.* 1990; Harkness *et al.* 2002) and lack the ability to effectively assemble chromatin *in vitro*, as well as properly regulate histone post-translational modifications (Harkness *et al.* 2002, 2005; Arnason *et al.* 2005; Harkness 2005; Turner *et al.* 2010; Islam *et al.* 2011). The compilation of defects observed in APC mutants manifest as reduced lifespan in yeast and mice (Baker *et al.* 2004; Harkness *et al.* 2004). The yeast FOXO family members Fkh1 and Fkh2 may play a role in APC-dependent lifespan regulation. The yeast APC appears to respond to signals from Fkh1 and Fkh2 to regulate yeast replicative and chronological lifespan (RLS and CLS, respectively), as well as stress response (Postnikoff *et al.* 2012). The Fkh proteins drive the expression of histones (Zhu *et al.* 2000), and when histone metabolism is defective, reduced yeast and worm lifespan results (Dang *et al.* 2009; Feser *et al.* 2010; Greer *et al.* 2011; Han and Brunet

2012). Consistent with a role for the APC in histone metabolism and lifespan, human cancer cells are continually being described that express aberrant APC activity (reviewed in Wäsch *et al.* 2010; Smolders and Teodoro 2011; Chan *et al.* 2012; Wang *et al.* 2013). A notable example of this is securin, a major APC substrate found elevated in many cancers that often serves as a prognostic marker of cancer recurrence (Smith *et al.* 2010; Lewy *et al.* 2012). Cancer and reduced lifespan are both tightly linked to genomic instability (McMurray and Gottschling 2004; Seviour and Lin 2010). In the work presented here, we investigate a specific molecular longevity network regulated by the APC.

Molecular mechanisms involved in determining lifespan in yeast have been heavily studied, with Fob1 being identified as an important player (Sinclair and Guarente 1997; Defossez *et al.* 1999; Zuin *et al.* 2010; Kobayashi 2011a; Pan 2011). Fob1 binds the replication fork barrier site (RFB), a specific sequence within rDNA tandem repeats (Mohanty and Bastia 2004), and unidirectionally blocks and stalls DNA replication forks (Kobayashi and Horiuchi 1996; Kobayashi *et al.* 1998). The stalled replication machinery can result in double-stranded DNA breaks (DSBs). Due to the repeated structure of rDNA, homologous DNA repair of rDNA DSBs can result in unequal sister chromatid exchange (USCE) generating substantial genomic instability within the rDNA region (Sinclair *et al.* 1997; Kobayashi *et al.* 1998; Ide *et al.* 2010). DSBs, resulting from stalled DNA replication forks, and USCE within the rDNA region, may be a conserved process (Mohanty *et al.* 2009; Ganley *et al.* 2009).

In contrast to its role in rDNA destabilization, the Fob1 protein also anchors genomic stabilizing factors such as rDNA-specific cohesins, condensins, and Sir2 within the nucleolus via interaction with the RENT (**re**gulators of **n**ucleolar silencing and **t**elophase exit) complex (Straight *et al.* 1999; Huang and Moazed 2003; Kobayashi and Ganley 2005; Huang *et al.* 2006; Johzuka and Horiuchi 2009). Furthermore, the RENT complex also sequesters the important phosphatase Cdc14 within the nucleolus in a cell-cycle-dependent manner. Interestingly, mice lacking the Cdc14b ortholog show early signs of aging (Wei *et al.* 2011). Taken together, Fob1 plays a multifaceted role in ensuring cellular health and longevity.

In this study we describe a yeast two-hybrid screen, in which the APC subunit Apc5 was used as bait, and we identified Fob1 as a binding partner. One possible outcome of this interaction is that the APC targets Fob1 for proteasome- and ubiquitin-dependent degradation. This would provide a molecular mechanism to explain how the APC controls lifespan and how the cell overcomes Fob1's potential negative effects on rDNA recombination and longevity. Recent work has demonstrated that the APC is required for rDNA silencing, assembly, and segregation in budding and fission yeast (Sullivan *et al.* 2008; Dubey *et al.* 2009; Rodríguez-Sánchez *et al.* 2011). Thus, the identification of Fob1 as a novel APC target would provide insight into how the APC may influence rDNA biology. Here we present a molecular mechanism depicting how the APC may regulate the maintenance of genomic stability and consequently longevity, at least in part through the degradation of Fob1.

Materials and Methods

Yeast strains

Table 1 lists the yeast strains used in this study. All strains were S288c derivatives unless stated otherwise. Standard genetic techniques, such as genetic crosses and homologous integration of PCR fragments, were performed to generate the strains listed, as previously described (Turner *et al.* 2010; Postnikoff *et al.* 2012). All other strains were obtained from the sources shown.

Media and methods

Media were prepared as previously described (Ausubel *et al.* 1995). Yeast cells were grown either in YPD (1% yeast extract, 2% peptone, 2% glucose) or synthetic defined (SD) media lacking the appropriate amino acids [1.7 g/liter yeast nitrogen base, 5 g/liter $(NH_4)_2SO_4$, 1.3 g/liter drop-out powder minus appropriate amino acids, and 1 tablet NaOH]. Glucose, galactose, or sucrose were used at a final concentration of 2%. *Escherichia coli* strains JM109 and DH10B were used to propagate DNA plasmids. DNA manipulations such as restriction enzyme digests, DNA minipreps, yeast and *E. coli* transformations, and yeast genomic DNA preparation were carried out according to standard protocols (Ausubel *et al.* 1995). Spot dilution assays were conducted by pipetting 5 μl of cells from samples generated from a 10-fold dilution series onto the various media shown and grown at the temperatures indicated. The starting spot generally contained 5×10^4 cells. For cell cycle arrest experiments, cells were considered arrested once >90% of the cells were in the desired phase of the cell cycle according to bud morphology. For interest sake, cells acquired from Research Genetics (ResGen) lacking *CDH1* arrested in G1 using α-factor (data not shown). Hydroxyurea (S phase arrest) and nocodazole (mitotic arrest) were used at 5 μg/ml and 0.3 M, respectively, for 2 hr to reach >90% synchronization. For α-factor arrest, 4 μg/ml in YPD at pH 3.5 was used for *BAR1* cells. Typically, 2 μg/ml was added and then 1 hr later, a second aliquot of 2 μg/ml was added. Arrest generally required 2–3 hr. For *bar1*Δ cells, 50 ng/ml for 3 hr was necessary. To stop protein synthesis, we used 10 μg/ml cycloheximide (CHX).

Two-hybrid screen

Full-length *APC5* was cloned into the two-hybrid bait plasmid pGBT9. pGBT-*APC5* was functional as it suppressed the *apc5*^{CA} *ts* growth phenotype (data not shown). The two-hybrid strain PJ69-4A (generously provided by E. Craig) was transformed with pGBT-*APC5*. Transformants were then transformed with a library of yeast fragments (0.5 to 2–3 kb) ligated into the prey vectors pGAD-C1, pGAD-C2, and pGAD-C3 (the library was kindly provided by E. Craig; see James *et al.* 1996 for details). The three pGAD vectors represent the three different

Table 1 Strains used in this study

Strain	Genotype	Source/reference
YTH3	*MATα ade2 leu2-3 lys2Δ201 ura3-52*	Harkness *et al.* 2005; W. Neupert
YTH5	*MATα ade2 his3Δ200 lys2Δ201 ura3-52*	Harkness *et al.* 2002
YTH6	*MAT***a** *ade2 his3Δ200 lys2Δ201 ura3-52*	Harkness *et al.* 2005
YTH225 (PJ69-4A)	*MAT***a** *trp1-901 leu2-3 ura3-52 his3-200 gal4Δ gal80Δ LYS2::GAL1-HIS3 GAL2-ADE2 met2::GAL7-lac*	E. Craig
YTH457	*MAT***a** *ade2 his3 leu2 ura3 apc5^{CA}*	Harkness *et al.* 2002
YTH1029	*MAT***a** *his3Δ1 Δleu2 Δmet15 Δura3*	Research Genetics (ResGen)
YTH1033	*MAT***a** *his3Δ1 Δleu2 Δmet15 Δura3 apc10::KanMX6*	ResGen
YTH1037	*MAT***a** *his3Δ1 Δleu2 Δmet15 Δura3 fob1::KanMX6*	ResGen
YTH1235	*MAT***a** *ade2 his3 leu2 lys2 ura3*	Harkness *et al.* 2004; isogenic with YTH5/6
YTH1636	*MAT***a** *ade2 his3 leu2 lys2*(?) *ura3*	Harkness *et al.* 2004
YTH1637	*MATα ade2 his3 leu2 lys2*(?) *ura3 apc5^{CA}*-PA::*His5*	Harkness *et al.* 2004
YTH1693	*MATα ade2 his3 leu2 ura3 apc10::KanMX6*	This study
YTH2425	*MAT? ade2 his3 leu2 lys2*(?) *ura3*	This study
YTH2454	*MAT? ade2 his3 leu2 ura3 fob1::KanMX6*	This study; seven backcrosses with YTH5/6
YTH2456	*MAT? ade2 his3 leu2 ura3 lys2*(?) *apc5^{CA}*-PA::*His5^{+} fob1::KanMX6*	This study
YTH3175	*MAT? ade2 his3 leu2 ura3 lys2*(?) *apc5^{CA}*-PA::*His5^{+} fob1::KanMX6*	This study
YTH3179	*MAT? ade2 his3 leu2 ura3 fob1::KanMX6*	This study
YTH3181	*MAT? ade2 his3 leu2 ura3 lys2*(?) *apc5^{CA}*-PA::*His5^{+} fob1::KanMX6*	This study
YTH3334	*MAT? ade2 his3 leu2 ura3 apc10::KanMX6 fob1::KanMX6*	This study
YTH3335	*MAT? ade2 his3 leu2 ura3 apc10::KanMX6 fob1::KanMX6*	This study
YTH3367	*MAT? ade2 his3 leu2 ura3 apc10::KanMX6*	This study
YTH3638	ResGen, but *MATα*, *rpn10:: KanMX6*	W. Xiao
YTH3785	ResGen, but *cdh1:: KanMX6*	W. Xiao
YTH3863	W303, *cdc20-1*	A. Ghavidel
YTH3880	*MAT***a** *his3 leu2 met15 ura3 APC5-TAP::HIS3*	A. Ghavidel
YTH4001	as YTH1235, but *bar1::KanMX6*	This study
YTH4004	as YTH457, but *bar1::KanMX6*	This study
YTH4028	as YTH5, but *APC5-TAP::HIS3*	This study
YTH4104	as YTH4001, but *FOB1-TAP::HIS3*	This study
YTH4267	*MATα ade2 his3 leu2 ura3*	This study; YTH3 × 6
YTH4269	*MATα ade2 his3 leu2 ura3*	This study; YTH3 × 6
YTH4414	*MAT? ade2 his3 leu2 ura3*	This study
YTH4415	*MAT? ade2 his3 leu2 ura3 fob1::KanMX6*	This study
YTH4416	*MAT? ade2 his3 leu2 ura3 apc5^{CA}*-PA::*His5^{+}*	This study
YTH4417	*MAT? ade2 his3leu2 ura3 apc5^{CA}*-PA::*His5^{+} fob1::KanMX6*	This study
YTH4422	CCFY100 triple silencer	K. Runge
YTH4444	as 4422, but *apc5^{CA}*-PA::*His5^{+}*	This study
YTH4447	as 4422, but *fob1::KanMX6*	This study
YTH4450	as 4422, but *apc5^{CA}*-PA::*His5^{+} fob1::KanMX6*	This study
YTH4519	as 4267, but *FOB1^{DB1}-TAP::HIS3*	This study
YTH4520	as 4267, but *FOB1^{E420V}-TAP::HIS3*	This study
YTH4525	as 4267, but *FOB1-TAP::HIS3*	This study
YTH4539	as 3638 (*rpn10Δ*), but *FOB1-TAP::HIS3*	This study
YTH4540	as 3638 (*rpn10Δ*), but *FOB1^{DB1}-TAP::HIS3*	This study
YTH4541	as 3638 (*rpn10Δ*), but *FOB1^{E420V}-TAP::HIS3*	This study

reading frames. A combination of all three libraries was used to transform pGBT-*APC5*-expressing PJ69-4A cells. Transformants were grown on SD −trp −leu plates to select for pGBT-*TRP1* and pGAD-*LEU2*-containing cells. Roughly 50,000 colonies were recovered on each of 30 separate transformation plates, for a total of ~1,500,000 transformants. After 2–3 days of growth, the plates were replica plated to SD −trp −leu −ade and SD −trp −leu −his plates to select for interactions with Apc5. Colonies required 1–3 weeks to grow on the triple drop-out plates. Positives grew on both sets of selection plates. A total of 80 positives were recovered from the screen. Plasmids were recovered from 36 of the positives and sequenced. The plasmids were called RIN, for ***R****MC1* **in**teracting. Cloning of *RMC1* proved it to encode Apc5 (Harkness *et al.* 2002). Two types of plasmids were recovered. First, as expected, plasmids in which gene coding sequences were fused in-frame to the *GAL*-activation domain were recovered. This group included *FOB1* and *CIN5*, which were recovered twice each, and *SRS2*, *IQG1*, *RMD7*, and *GAL1*, which were each recovered once. Iqg1 was recently shown to be ubiquitinated by the APC

(Ko *et al.* 2007). The second group of unexpected sequences included the promoter regions of a select number of genes. This set included the intergenic region between *MATalpha1* and *BUD5* (recovered 14 times), the *TUP1* promoter (recovered 5 times), and the promoters to *SSN6*, *PEX28*, *PRP2*, and *RDN25-2* (each recovered once). We suspect that this group of sequences represents a one-hybrid type of interaction where Apc5 recruits a transcription factor to the *GAL* promoter, that when bound to these pGAD-based sequences, is capable of driving the transcription of the reporter gene.

Plasmids

The plasmids used in this study are shown in Table 2 and the primers used to generate each construct are shown in Table 3. *FOB1* was cloned into the two-hybrid prey vector, pGAD·C2 (kindly provided by E. Craig, University of Wisconsin), by first cloning a full-length *FOB1* PCR fragment into the pCR4-TOPO cloning vector (Invitrogen). Primers 1 and 2 (from Table 3) were used in PCR reactions with wild-type genomic DNA (gDNA) as template. Topo-*FOB1* was then digested with *Bam*HI and *Sal*I, as *Bam*HI and *Sal*I sites were embedded within the 5′ and 3′ primers, respectively. This fragment was then cloned into *Bam*HI/*Sal*I digested pGAD·C2. Domain 1 (D1) was cloned by digesting pGAD-*FOB1* with *Pst*I, followed by religation. *Pst*I digested at nucleotide 299 within *FOB1* and within the multiple cloning site downstream of the *FOB1* stop. Domain 2 (D2) was cloned by using primers 1 and 3 in PCR reactions using wild-type gDNA as template. The PCR fragment was cloned into pCR4-TOPO and topo-$FOB1^{D2}$ was digested with *Bgl*II and *Pst*I. A *Pst*I site was embedded within the PCR fragment at nucleotide 299. The *Bgl*II/*Pst*I fragment was cloned into *Bgl*II/*Pst*I digested pGAD·C2. Domains 1 and 2 (D1/2) were cloned by digesting topo-$FOB1^{D2}$ with *Bam*HI/*Bgl*II, which was ligated into *Bam*HI digested pGAD·C2. Domain 3 (D3) was cloned by using primers 2 and 4 in PCR reactions with wild-type gDNA as template. The PCR fragment was cloned into pCR4-TOPO. Both topo-$FOB1^{D3}$ and pGAD·C2 were digested with *Bam*HI and *Sal*I and the appropriate fragments were ligated together. The N-term fragment was cloned by using primers 1 and 5 in PCR reactions with wild-type gDNA as template. The resultant fragment was cloned into pCR4-TOPO. Topo-$FOB1^{N\text{-}term}$ and pGAD·C2 were digested with *Bam*HI and *Sal*I and the appropriate fragments were ligated together. Finally, the C-term fragment was cloned using primers 2 and 6 in PCR reactions. The fragment was cloned into pCR4-TOPO. Topo-$FOB1^{C\text{-}term}$ and pGAD·C2 were digested with *Bam*HI and *Sal*I and the appropriate fragments were ligated together.

The Fob1 L box E420V mutation was created using a PCR-based method to direct homologous recombination within yeast cells (Ito *et al.* 2008). Approximately 35 nucleotides of homology allowed two PCR fragments to recombine with each other or with a plasmid backbone. The primers used are listed in Table 3. To create the E420V mutation within the L box, primers 1 and 7 generated product A, while primers 2 and 4 generated product B, using wild-type gDNA as a template. Products A and B overlapped by 32 nucleotides, 1259–1291. The GAL_{pro}-*FOB1-HA* plasmid was digested with *Cla*I, which specifically removed *FOB1* base pairs (bp) 556 to 1369. Thus, there were 556 bp of homology between the backbone and PCR product A, and 332 bp of homology between PCR product B and the backbone. The three linear fragments were transformed together into YTH1029, the Research Genetics wild-type strain, and transformants were selected on SD −URA. YTH1029 seemed to have a high recombination rate, producing more recombined plasmids than our other wild-type strains. Transformants were scraped off the plates and resuspended into 2 ml of SD −URA liquid. Total DNA was extracted using a "smash and grab" technique (Ausubel *et al.* 1995; Harkness *et al.* 2002) and electroporated into DH5α *E. coli* cells. Since the new restriction site introduced into the L box mutation, *Acl*I, was blocked by CpG methylation, all recovered plasmids were also transformed into *E. coli* K12 cells that contain a dam-3 mutation and are defective in adenine methylation (Marinus and Morris 1975), allowing restriction of *Acl*I sites.

Westerns

For crude yeast whole-cell protein extraction, yeast cultures were grown in 5–10 ml of the appropriate media at the required temperature to an OD_{600} of 1.0. The cells were then harvested and resuspended in a volume of SDS–PAGE loading dye containing 3% βME calculated according to the following equation: volume of dye (μl) = OD_{600} × volume of culture (ml) × 5. Resuspended samples were boiled for 5 min, after which cellular debris was pelleted at 14,000 rpm for 5 min and discarded. For arrest/release experiments, protein lysates were prepared according to a TCA-based method. Briefly, 3-ml samples were removed at the indicated time points. The cells were pelleted and resuspended in 240 μl 1.85 M NaOH/7.4% β-mercaptoethanol. After a 5-min incubation on ice, 240 μl of 100% trichloroacetic acid (TCA) was added, followed by another 5-min incubation on ice. The sample was centrifuged for 10 min, the supernatant was removed, and the pellet was gently washed with H_2O. The pellet was then resuspended in 50 μl buffer A (13% SDS, 1 M unbuffered Tris) and 50 μl buffer B (30% glycerol, a small scoop of bromophenol blue powder) and stored at −80°. The samples were heated at 65° for 15 min prior to analyzing 5–10 μl by SDS–PAGE. Equalized samples, based on image analysis of load control protein bands using Image J 1.37v software (National Institutes of Health), were then transferred to nitrocellulose membrane. For Western analysis, the membranes were blocked in 5% nonfat milk (Biorad) and PBST overnight at 4°. The membranes were then incubated with primary antibody in 5% nonfat milk and PBST for 1.5 hr at room temperature or overnight at 4°. The membranes were then washed three times in PBST for 15 min and incubated in 1:10,000 dilution of secondary antibody in 5% nonfat milk and PBST for 1 hr at room temperature. After another three washes in PBST for 15 min, the membranes were processed with enhanced chemiluminescence

Table 2 Plasmids used in this study

Plasmid	Markers	Source/reference
pVA3	p53 2μ-*TRP1* 2 hyb·$GAL4_{BD}$	W. Neupert
pTD1	SV40 large T-antigen 2μ-*LEU2* 2 hyb·$GAL4_{AD}$	W. Neupert
pGBT9	2μ-*TRP1* 2 hyb·$GAL4_{BD}$	W. Neupert
pGBT-*APC5*	2μ-*TRP1* 2 hyb·$GAL4_{BD}$	This study
YCp50	*CEN-URA3*	W. Neupert
pTH54	YCp50-$APC5^{\Delta 3'69}$	Harkness *et al.* 2002
YEplac195-*FOB1*	2μ-*URA3*	T. Kobayashi
pGAD·C2	2μ-*LEU2* 2 hyb·$GAL4_{AD}$	E. Craig
pRIN12, 20	$FOB1^{5\text{-}1263}$ 2μ-*LEU2* 2 hyb·$GAL4_{AD}$	This study
pCR4-TOPO	Bacterial PCR cloning vector	Invitrogen
topo-*FOB1*	pCR4-TOPO	This study
pGAD-*FOB1*	2μ-*LEU2* 2 hyb·$GAL4_{AD}$	This study
pGAD-$FOB1^{D1}$	2μ-*LEU2* 2 hyb·$GAL4_{AD}$	This study
topo-$FOB1^{D2}$	pCR4-TOPO	This study
pGAD-$FOB1^{D2}$	2μ-*LEU2* 2 hyb·$GAL4_{AD}$	This study
topo-$FOB1^{D3}$	pCR4-TOPO	This study
pGAD-$FOB1^{D3}$	2μ-*LEU2* 2 hyb·$GAL4_{AD}$	This study
pGAD-$FOB1^{D1/2}$	2μ-*LEU2* 2 hyb·$GAL4_{AD}$	This study
topo-$FOB1^{N\text{-}term}$	pCR4-TOPO	This study
pGAD-$FOB1^{N\text{-}term}$	2μ-*LEU2* 2 hyb·$GAL4_{AD}$	This study
topo-$FOB1^{C\text{-}term}$	pCR4-TOPO	This study
pGAD-$FOB1^{C\text{-}term}$	2μ-*LEU2* 2 hyb·$GAL4_{AD}$	This study
pBG1805	GAL_{pro}.6X His·HA·Prot A 2μ-*URA3*	W. Xiao
GAL_{pro}-*FOB1-HA*	GAL_{pro}.6X His·HA·Prot A 2μ-*URA3*	W. Xiao
GAL_{pro}-$FOB1^{E420V}$-*HA*	GAL_{pro}.6X His·HA·Prot A 2μ-*URA3*	This study
GAL_{pro}-$FOB1^{DB1}$-*HA*	GAL_{pro}.6X His·HA·Prot A 2μ-*URA3*	This study
GAL_{pro}-$FOB1^{DB2}$-*HA*	GAL_{pro}.6X His·HA·Prot A 2μ-*URA3*	This study
GAL_{pro}-$FOB1^{DB1/DB2}$-*HA*	GAL_{pro}.6X His·HA·Prot A 2μ-*URA3*	This study
pYEX-*APC5-GST*	*URA3/AMP CuP*	This study
pPAS-*ADE2*	*CEN-ADE2*	W. Xiao

reagent (PerkinElmer) and exposed to Kodak film. Antibodies against HA, TAP, and GAPDH were purchased from Abcam.

Lifespan determination

Replicative, or generational, lifespan (RLS) of the strains tested in this study was based on previously published protocols (Kennedy *et al.* 1994; Harkness *et al.* 2004; Postnikoff *et al.* 2012). Briefly, cells from fresh overnight cultures were struck out onto the appropriate media prepared fresh. The plates were then grown overnight at 30°. The next day, ~30 cells containing small buds were micromanipulated to isolated areas of the plate. The small daughter buds were kept as the starting mother cells. All additional buds from the starting mother cells were scored and discarded. The plates were kept at 30° during working hours and stored at 4° overnight. Statistical significance of differences among RLS was determined using the nonparametric Mann–Whitney *U*-test with IBM SPSS Statistics 21 software. Mean lifespan, which is the number of divisions reached by 50% of the mother cells, was calculated with Microsoft Excel using the formula =FORECAST (X, known Ys, known Xs) when data points corresponding to 50% viability were not available. When this formula was used, X was 50, corresponding to the desired mother cell viability (50%), "known Ys" were the number of mitotic divisions corresponding to the data points immediately above and below 50%, while "known Xs" were the viability percentages of available data points directly above and below 50%.

Determination of rDNA recombination frequency and plasmid loss

A strain containing a phenotypic marker (the *CAN1-ADE2* cassette) cloned into the rDNA locus was used to measure the recombination frequency within the rDNA region (kindly provided by K. Runge; Roy and Runge 2000). This strain forms red colonies instead of white when this cassette is lost due to recombination within the rDNA locus. The ratio of red to white colonies is representative of rDNA recombination frequency. Similarly, the loss of an empty vector *CEN-ADE2* plasmid in nonselective media results in red *vs.* white colonies and is an approximate measure of chromosome loss, which is representative of global genomic instability. An overnight culture grown in YPD to an OD_{600} of 1.0, inoculated by an individual white colony, was serially diluted to ~500 colony-forming units (CFUs)/plate and plated on YPD. Similarly, colonies harboring the *CEN-ADE2* plasmid, picked off of selective plates, were grown in nonselective YPD overnight to an OD_{600} of 1.0, then diluted and plated on YPD. Plates were grown for 4–7 days to allow red color formation in recombinants. Red and total CFUs were counted. Sectored colonies were excluded from the recombinant count so to only measure *CAN1-ADE2* cassette loss during overnight growth in

Table 3 Primers used in this study

	Primer name	Primer sequence	Imbedded RE
1	GAD·Fob1·5′	5′–ATGCTA GGATCC AC ^{4}ACGAAACCGCGTTACAATG^{22}	*Bam*HI
2	GAD·Fob1·3′	5′–ATGCTA GTCGAC ^{1701}TTACAATTCCATTGATGTG^{1683}	*Sal*I
3	Fob1·Dom2·3′	5′–ATGCTA AGATCT A ^{1258}CATTAGCAAGGGCAAAAG^{1241}	*Bgl*II
4	Fob1·Dom3·5′	5′–ATGCTA GGATCC ^{1259}AAGCGGATAATAGCTGTAAC^{1278}	*Bam*HI
5	Fob1·N-term·3′	5′–ACGT GTCGAC ^{849}AATTGGAACCCTAGCAAATG^{829}	*Sal*I
6	Fob1·C-term·5′	5′–ACGT GGATCC ^{850}ACTTCGTAACATCAAGCATCTTA G^{868}	*Bam*HI
7	E420V 3′	5′–ACGTACGTG^{1291}GAATTC CATTATTGTTACAGCTATTATCCGCAAC**g**TTAGCAAGGG^{1247}	*Eco*RI/*Acl*I

The underlined sequences reflect restriction sites imbedded for cloning purposes. The nucleotide in bold in primer 7 was mutated to create the E420V mutation, which also created the new AclI restriction site. The superscript numbers within the primer sequences define where in the FOB1 DNA sequence the primers reside.
RE, restriction enzyme.

liquid culture, rather than recombination events that occurred after plating. Likewise, by counting only red colonies in the *CEN-ADE2* experiment, only loss events that occurred in liquid culture prior to plating were considered. Recombination and plasmid loss frequency was expressed as the number of red CFUs/10^4 cells. The experiments were done at least in triplicate. Standard error of the mean is shown.

Results

Identification of Fob1 as an Apc5 binding partner in a yeast two-hybrid screen

In an effort to identify novel APC substrates, regulators, and/or modifiers we conducted a yeast two-hybrid screen using the APC subunit Apc5 as bait. Two prey plasmids encoding *FOB1* nucleotides 5–1263 were recovered in this screen. Considering the involvement of the APC and Fob1 in yeast lifespan (Harkness *et al.* 2004; Harkness 2006; Kobayashi 2011a,b; Postnikoff *et al.* 2012), we focused on whether the Apc5/Fob1 interaction defined a molecular mechanism for APC-dependent longevity. Specifically, we investigated whether the yeast two-hybrid interaction defined Fob1 as an APC substrate, through which RLS could be controlled.

Deletion of FOB1 in APC mutants has little impact on growth, but a positive influence on APC mutant RLS

We first tested genetic interactions between *FOB1* and *APC5* with regard to growth and RLS. We deleted *FOB1* in *apc5^{CA}* and *apc10*Δ cells to ask whether this restored *apc5^{CA}* or *apc10*Δ associated *ts* growth phenotypes. Our spot dilution results show that deletion of *FOB1* had little impact on *apc5^{CA} ts* growth and mildly suppressed *apc10*Δ *ts* growth (Figure 1, A and B). Removal of *FOB1* from the cell had little benefit on growth in cells harboring an impaired APC.

Next, we asked whether *FOB1* deletion was of any benefit to *apc5^{CA}*- or *apc10*Δ-defective RLS, a measure of how many daughter cells a single mother will produce prior to senescence (Kennedy *et al.* 1994). If lower levels of Fob1 promote increased lifespan, and if the APC facilitates the reduction of Fob1, then deletion of *FOB1* may restore reduced RLS in APC mutants. Our results indicate that deletion of *FOB1* increased both *apc5^{CA}* and *apc10*Δ RLS (Figure 1, C and D). The mean lifespans of each mutant RLS were significantly different from WT with *P*-values less than 0.05. This data implies that the growth and RLS defects of APC mutants are broad in range and are not solely due to excess Fob1. However, the RLS data do provide support for our theory that the APC regulates lifespan, at least in part, by affecting Fob1 protein levels.

Increased FOB1 expression can be toxic to cells and reduce RLS

We assessed the effects of increased *FOB1* expression on RLS and cell cycle progression. Increased *FOB1* expression, via a 2μ plasmid, reduced RLS in WT cells (Figure 2A). The mean RLS of WT cells expressing *FOB1* is significantly different from the RLS of cells expressing the empty vector (EV) with a *P*-value <0.05. Increased *FOB1* expression in *apc5^{CA}* cells, on the other hand, did not reduce RLS any further. One possible explanation is that Fob1 levels may already be elevated in *apc5^{CA}* cells, such that any further Fob1 protein increase had no additional negative impact on RLS. Furthermore, it is also possible that increased expression of *FOB1* may disrupt complexes that regulate rDNA, such as RENT, reducing RLS.

Overexpression of *FOB1* via the *GAL$_{pro}$-FOB1-HA* construct impaired the growth of WT and *apc5^{CA}* cells (Figure 2B). The effect was greater in *apc5^{CA}* cells. Fob1 expression from the 2μ plasmid, as opposed to that from the *GAL* promoter, did not impair WT or *apc5^{CA}* growth, suggesting Fob1 accumulates to a larger degree when expressed from the *GAL* promoter. The slow growth in the presence of excess Fob1 suggests the removal of Fob1 may be required for efficient cell cycle progression.

To test whether Fob1 levels are indeed elevated in *apc5^{CA}* cells, we expressed Fob1-HA from a *GAL*-inducible promoter for 6 hr in WT and *apc5^{CA}* asynchronous cells and removed samples every hour to observe Fob1-HA induction (Figure 2C). After the 6-hr induction, the cells were washed and resuspended in 2% glucose, with samples taken every hour for flow cytometry and Western analysis (Figure 2D). CHX was not used to block protein synthesis in this experiment to observe whether increased Fob1 protein levels impacted cell cycle progression. We show that Fob1-HA accumulated faster, and was degraded slower, in *apc5^{CA}* cells compared to WT cells (Figure 2, C and D). The flow cytometry data shows that overexpression of *FOB1* caused cell populations to accumulate in G1. WT cells reentered the cell cycle within 2 hr, whereas *apc5^{CA}* cells were delayed, requiring 6 hr (Figure 2D). It is unlikely that Fob1 accumulation in *apc5^{CA}* cells is solely responsible for delayed reentry into the cell cycle since

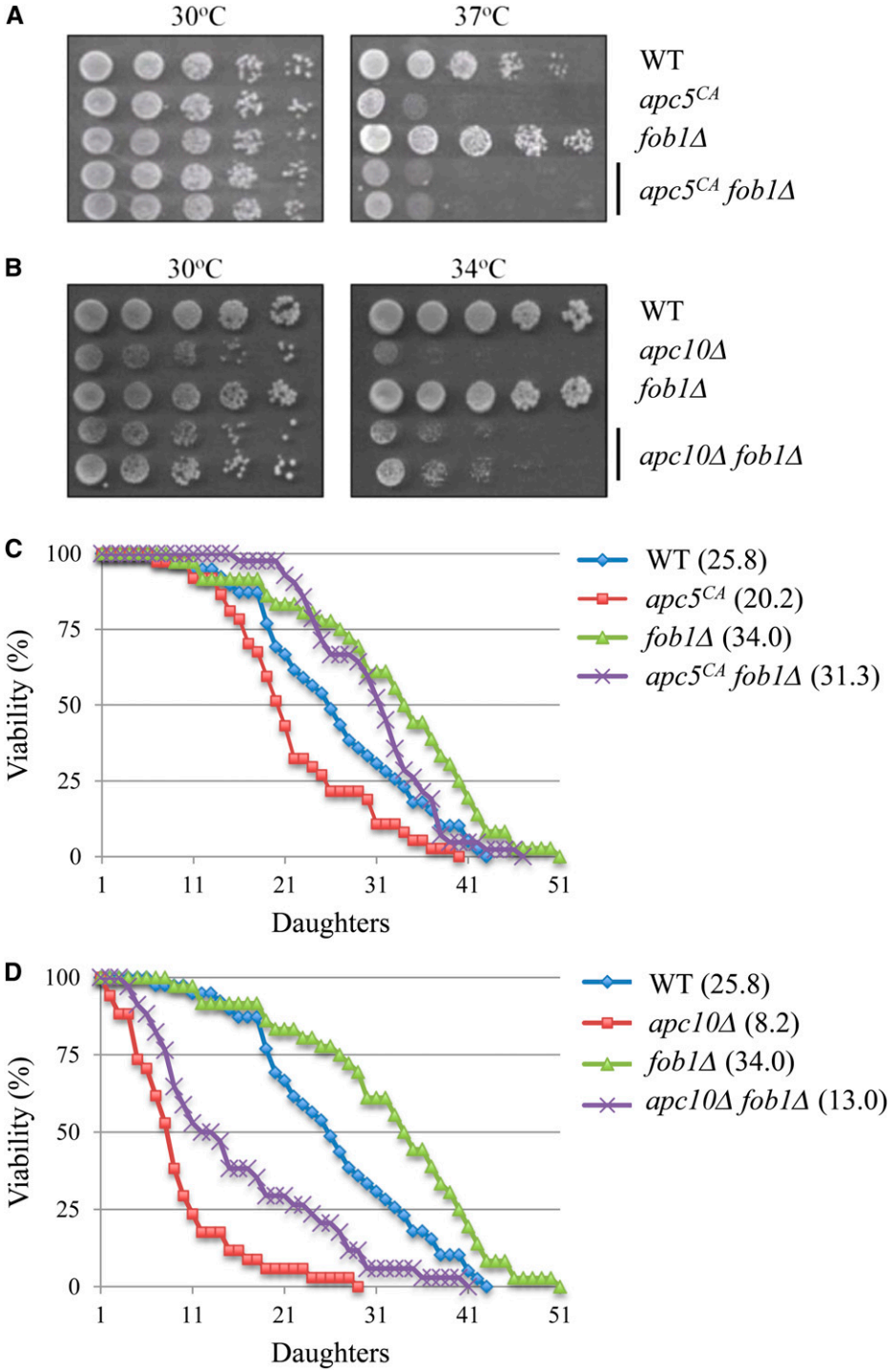

Figure 1 Deletion of *FOB1* in APC mutants has little impact on growth, but a positive influence of APC mutant RLS. (A) WT, *apc5*^{CA}, *fob1Δ*, and *apc5*^{CA} *fob1Δ* cells were grown to an OD_{600} of 0.5, then 10-fold serially diluted and spotted onto YPD plates. The plates were incubated at 30° and 37° for 3 days. (B) WT, *apc10Δ*, *fob1Δ*, and *apc10Δ fob1Δ* cells were treated as above. (C) RLS for WT, *apc5*^{CA}, *fob1Δ*, and *apc5*^{CA} *fob1Δ* cells was determined. The numbers of mother cells used for RLS determination were 39, 37, 36, and 42, respectively. (D) RLS for WT, *apc10Δ*, *fob1Δ*, and *apc10Δ fob1Δ* cells was determined. The numbers of mother cells used for RLS determination were 39, 34, 36, and 34, respectively. The mean RLS for panels C and D are shown in parentheses. Mean RLS was determined using the formula =FORECAST in Excel, as described in *Materials and Methods*. Statistical significance of differences for each RLS relative to WT was determined using the nonparametric Mann–Whitney *U*-test. Differences are considered significant, as each *P*-value is <0.05.

apc5^{CA} cells have broader defects. Nonetheless, these data support a model that shows dependence upon reduction of Fob1 levels during G1, possibly mediated by the APC that permits cell cycle progression into S phase.

Deletion of FOB1 alleviates cell cycle and rDNA recombination defects in apc5^{CA} *cells*

Genetic interactions between the APC and *FOB1* are also apparent with regard to cell cycle profiles (Figure 3, A and B) and ribosomal DNA (rDNA) recombination frequency (Figure 3D). Using flow cytometry to determine cell cycle profiles in asynchronous cells, we observed that >60% of *apc5*^{CA} cells accumulated in G2/M of the cell cycle (Figure 3A), as previously observed (Harkness *et al.* 2002; Arnason *et al.* 2005), whereas only 50% of the WT population was in G2/M. APC mutants have difficulty eliminating securin and cyclins, resulting in multiple defects in mitotic progression and an arrest at the metaphase/anaphase boundary (Zachariae and Nasmyth 1999). Indeed, the cyclin Clb2 was more abundant in *apc5*^{CA} cells compared to WT (Figure 3B). Interestingly, the

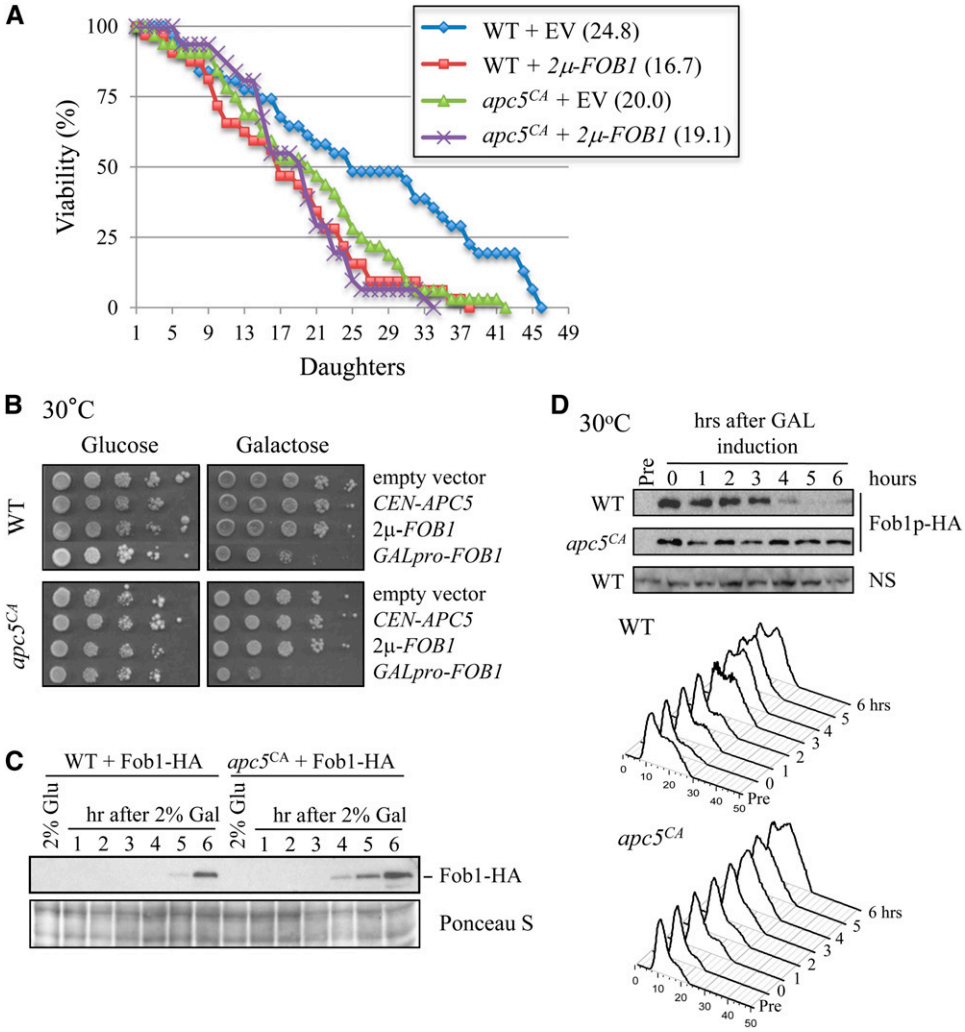

Figure 2 Increased *FOB1* expression reduces RLS while overexpression is toxic. (A) RLS determination for WT and *apc5*^{CA} cells harboring 2μ-*FOB1* or YCp50 empty vector. The number of mother cells used for WT + YCp50, WT + 2μ-*FOB1*, *apc5*^{CA} + YCp50, and *apc5*^{CA} + 2μ-*FOB1* were 31, 32, 32, and 31, respectively. Mean RLS is shown in parentheses. Differences from WT are statistically significant with *P*-values <0.05. (B) WT and *apc5*^{CA} cells harboring YCp50 empty vector, *CEN-APC5*, 2μ-*FOB1* or *GAL*$_{pro}$-*FOB1-HA* were serially diluted and spotted onto 2% glucose or 2% galactose-supplemented SD media. Plates were incubated at 30°, 3 days for glucose and 5 days for galactose plates. (C) WT and *apc5*^{CA} cells expressing *GAL*$_{pro}$-*FOB1-HA* were grown to early log phase, then induced with 2% galactose. Samples were taken every hour during the induction period and analyzed by Western blotting with antibodies against HA. The Ponceau S stained blot is shown for load control. (D) The cells used above were released into fresh 2% glucose media after the 6-hr galactose induction and allowed to reenter the cell cycle. Every hour for 6 hr, samples were removed for flow cytometry and Western analyses. NS, nonspecific band in WT cells.

deletion of *FOB1* in *apc5*^{CA} cells restored a WT cell cycle profile and reduced the accumulation of Clb2 in *apc5*^{CA} cells (Figure 3, A and B). One possible explanation for our data could involve rDNA segregation defects in *apc5*^{CA} cells due to slow or untimely cohesin cleavage, which is relieved in *fob1Δ* cells by the reduction of cohesin recruitment to the rDNA.

Considering the role Fob1 plays in rDNA metabolism, we tested whether *fob1Δ* genetically interacted with *apc5*^{CA} to regulate rDNA. Here we demonstrate a link between the APC, *FOB1*, and rDNA recombination, a process known to impinge on lifespan (Riesen and Morgan 2009; Kobayashi 2011a). Recombination events within the rDNA locus occur frequently relative to other regions in the genome, rendering this region a predominant source of genomic instability. Genomic instability in heterochromatic regions such as the rDNA and telomeres is correlated with decreased longevity (Kobayashi 2011a). Recombination events, such as USCE, can result in the loss of tandem rDNA repeats (Roy and Runge 2000; Kobayashi 2011b). We assessed the recombination frequency within the rDNA region by measuring the loss of a phenotypic marker cloned into an rDNA repeat (Figure 3C; the strain was a kind gift from K. Runge). Similarly, the loss of an empty vector *CEN-ADE2* plasmid in nonselective media is an approximate measure of chromosome loss and is representative of global genomic instability. Both *apc5*^{CA} (Figure 3D) and *apc10Δ* (data not shown) mutants had increased rDNA recombination frequency and plasmid loss (Figure 3E), indicating increased rDNA and global genomic instability. This is in agreement with the reduced RLS in APC mutants (Harkness *et al.* 2004; Postnikoff *et al.* 2012). Deletion of *FOB1* strongly reduced the recombination frequency and returned the frequency to WT levels in *apc5*^{CA} cells (Figure 3D). In contrast, the *apc5*^{CA} and *apc5*^{CA} *fob1Δ* cells had similar levels of plasmid loss (Figure 3E), indicating that Fob1 acts exclusively at the rDNA locus. This genetic interaction supports our hypothesis that the APC's role in maintaining genomic stability may be achieved, at least in part, through the degradation of Fob1 and maintenance of rDNA genomic stability.

Fob1 levels oscillate throughout the cell cycle and require APC^{Cdh1} *for turnover*

If Fob1 is indeed a target of the APC, presumably Fob1 protein levels fluctuate as the cell progresses through the cell cycle, as many known APC targets do. To test Fob1 cycling,

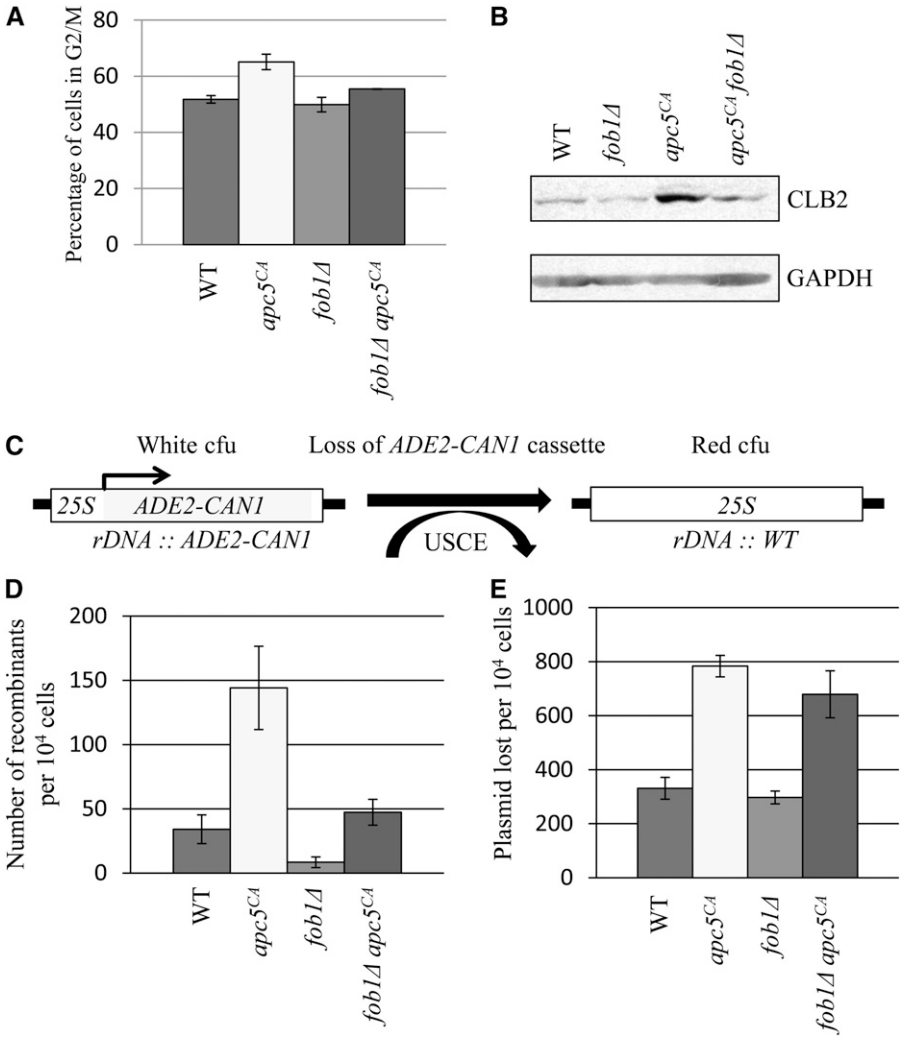

Figure 3 Deletion of *FOB1* alleviates cell cycle and rDNA recombination defects in *apc5^{CA}* cells. (A) Flow cytometry studies of steady state WT, *fob1Δ*, *apc5^{CA}*, and *apc5^{CA} fob1Δ* cells grown in YPD at 30°. (B) Western analyses of the cells used above with antibodies against Clb2 and GAPDH as a loading control. (C) Schematic of the *CAN1-ADE2* construct cloned into one of the 25S rDNA repeats and the corresponding recombinant WT form. The ratio between red colony forming units (CFUs) and total CFUs is a comparative measure of the frequency of recombination events within the rDNA locus. The strain was a generous gift from K. Runge. (D) The average frequency of recombination in the rDNA for five individual colonies of WT, *fob1Δ*, *apc5^{CA}*, and *apc5^{CA} fob1Δ*, as judged by the loss of the *ADE2* gene. Recombination frequency is expressed as the number of recombinant red CFUs per 10^4 cells. Standard error of the mean is shown. (E) The average frequency of plasmid loss for five individual colonies of WT, *fob1Δ*, *apc5^{CA}*, and *apc5^{CA} fob1Δ*, as judged by the loss of the *CEN-ADE2* plasmid. The frequency is expressed as the number of red CFUs per 10^4 cells. Standard error of the mean is shown.

we arrested cells harboring endogenous *FOB1-TAP* in G1 using the yeast α-factor pheromone. The cells were then washed and released into fresh YPD media lacking α-factor to allow synchronous cell cycle reentry. Samples were collected every 20 min for Western analysis to assess protein levels (Figure 4A) and flow cytometry to monitor cell cycle progression. Western analysis of TAP, Clb2 (a known APC target), and GAPDH as a loading control, showed that Fob1 protein levels were low in G1 and increased as the cells progressed to mitosis, resembling Clb2 cycling (Figure 4A). To determine whether Fob1 instability is a cell-cycle-specific event, we arrested Fob1-TAP cells in G1, M, and S phase using α-factor, nocodazole, or hydroxyurea, respectively. Following arrest, CHX was added and samples were removed every 30 min for Western analyses using antibodies against TAP and GAPDH. The results show that Fob1-TAP was predominantly unstable during G1 (Figure 4B). When *FOB1* was endogenously TAP tagged in *apc5^{CA}* cells, we observed that Fob1 stabilization during G1 was increased (Figure 4C). Residual Clb2 following G1 arrest was also stable in *apc5^{CA}* cells.

To establish whether Fob1 turnover relies on either the APC^{Cdc20} or the APC^{Cdh1} complex, we utilized cells expressing a mutation to *CDC20* or a deletion of *CDH1*, which encode temporal APC activators. The APC utilizes cell-cycle-specific adaptors that recruit substrates for ubiquitination and subsequent degradation (Barford 2011). The mitotic APC adaptor Cdc20 binds to the APC in G2 to promote the metaphase/anaphase transition. The APC adaptor Cdh1 binds the APC in late mitosis and promotes APC substrate degradation specific for mitotic exit and G1 maintenance. We therefore performed arrest/release experiments in *cdh1Δ* and *cdc20-1* cells expressing *GAL$_{pro}$-FOB1-HA*. The cells were grown in selection media containing 2% glucose to an OD_{600} of 0.5, after which α-factor was added to arrest cells in G1. After 2–3 hr, >90% of the cells were unbudded, as observed microscopically, and in G1, as determined by flow cytometry (data not shown). The cells were then washed and 2% Gal + α-factor was added for 4 hr to express the *FOB1* constructs while keeping the cells in G1. Next, the cells were washed and resuspended in 2% glucose and CHX to stop protein synthesis. We observed that Fob1-HA was stable over time in the absence of Cdh1, but not when Cdc20 was mutated (Figure 4D). Fob1-HA expression and stability in *cdc20-1* cells was at WT levels (compare with Fob1-HA expression in WT cells in Figure 7A). These

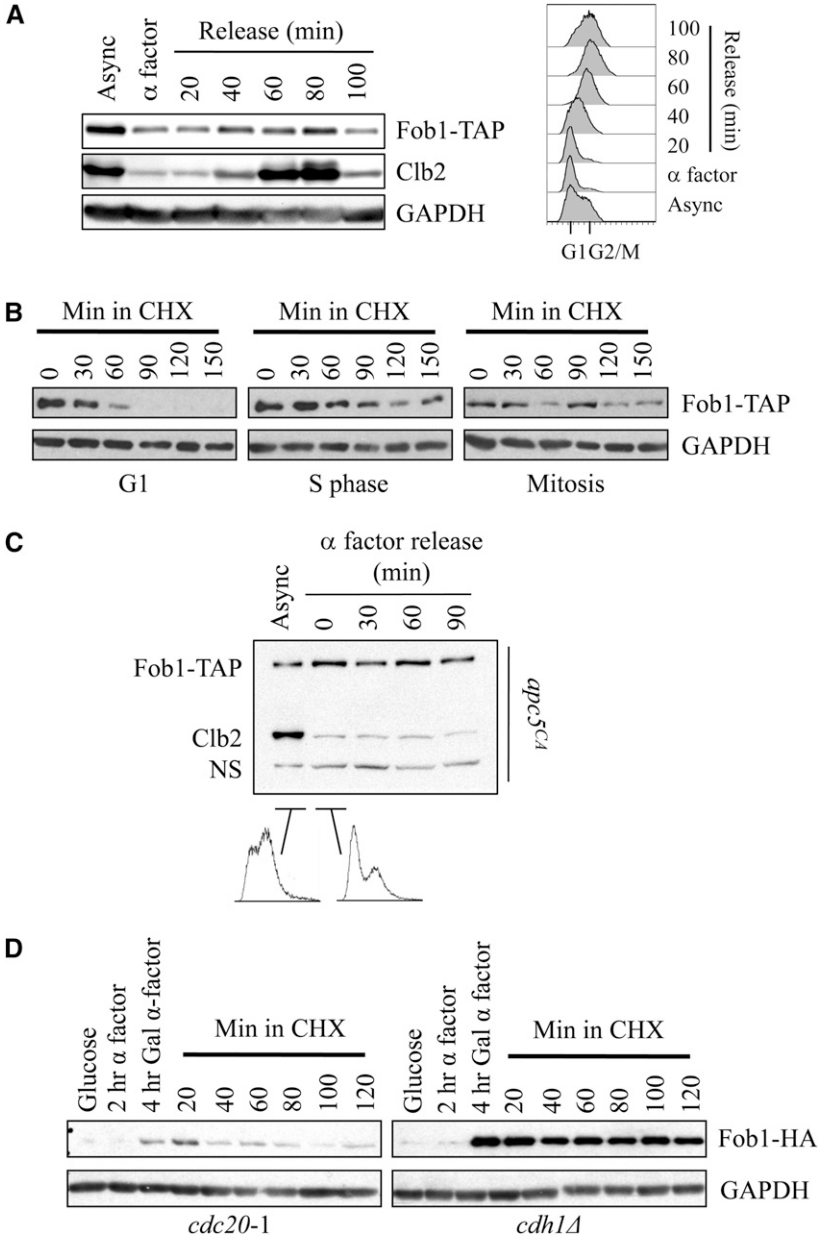

Figure 4 Fob1 oscillates throughout the cell cycle, is predominantly unstable during G1, and requires APC^{Cdh1} for turnover. (A) WT cells expressing endogenously tagged *FOB1-TAP* were arrested with α-factor, then washed and released into fresh media lacking α-factor. Samples were collected for flow cytometry and Western analyses every 20 min for 100 min. Westerns were performed using antibodies against TAP, Clb2, and GAPDH as a loading control. (B) WT cells expressing endogenous Fob1-TAP were arrested in G1 with α-factor, S phase with hydroxyurea, or mitosis using nocodazole. The cells were washed and resuspended in fresh media containing CHX to prevent further protein synthesis. Samples were removed every 30 min and analyzed by Western blotting with antibodies against TAP and GAPDH. (C) *apc5*^{CA} *FOB1-TAP* cells were arrested in G1 using α-factor. Flow cytometry was used to confirm arrest. Following arrest, the cells were resuspended in fresh media containing CHX. Samples were removed every 30 min for TAP and Clb2 Westerns. NS, nonspecific band. (D) *cdh1Δ* and *cdc20-1* cells expressing *GAL*$_{pro}$-*FOB1-HA* were arrested in G1 with α-factor, followed by induction of the *FOB1* construct with galactose. Cells were then washed and released into fresh media containing 2% glucose and CHX, with samples collected every 20 min for protein stability studies. Samples were analyzed using Westerns with antibodies against HA and GAPDH as a loading control.

results are in agreement with Fob1 protein levels peaking during mitosis with a subsequent APC^{Cdh1}-dependent drop in G1.

Identification of a Fob1 modified D box that is important for Apc5 binding in a yeast two-hybrid screen

To identify regions within Fob1 responsible for Apc5 interactions we subcloned *FOB1* fragments into the pGAD·C2 vector and tested interactions of these fragments with pGBT-*APC5* (Figure 5, A and B). The original *FOB1* clone we identified in the two-hybrid screen contained *FOB1* 5–1263 bp (Fob1 is 1701 bp long). *FOB1* gene fragments containing 1–299 bp (D1), 300–1258 (D2), 1259–1701 (D3), 1–1258 (D1/D2), or 1–849 (N half) did not interact with Apc5 in a yeast two-hybrid experiment. The only other fragments capable of interacting with Apc5 were the full-length *FOB1* gene and the 850–1701 (C term) fragment, which displayed a very weak interaction (Figure 5B). Based on the overlap of the fragments (Figure 5A), we concluded that *FOB1* 1259–1263 bp are important but not exclusive for this Fob1/Apc5 interaction, with additional motifs or structural features likely contributing to a fully robust interaction. Given that the main function of the APC is to target substrates for ubiquitin- and proteasome-dependent degradation, we tested the possibility that the Fob1/Apc5 interaction may define Fob1 as a bonafide APC substrate using a biochemical approach.

The putative Fob1 modified D box is required for Fob1 modification

APC substrates often encode a motif, or motifs, that are required for interaction with, and/or ubiquitination by, the APC. These motifs include the Destruction box (D box; **RXXL**XXXX**N**/**RXXL**), the KEN box, the A box, the CRY box,

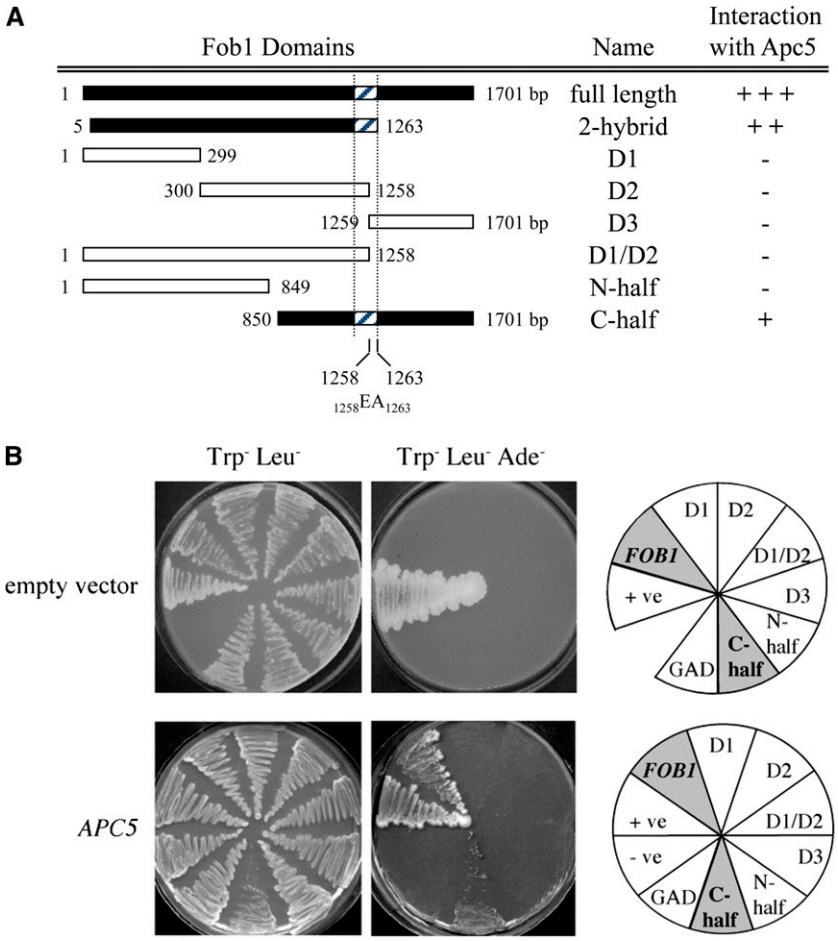

Figure 5 Apc5 interacts with Fob1 in a two-hybrid assay. (A) Schematic of the *FOB1* fragments cloned into pGAD·C2 to identify a Fob1 binding motif responsible for Apc5 interactions. +++ denotes best growth, + denotes weak growth, and − indicates no growth in a yeast two-hybrid assay. The hatched area denotes a putative Apc5 binding domain. (B) Growth analysis of *FOB1* derivatives and full-length *APC5* in a two-hybrid assay. Top panels show the *FOB1* derivatives (cloned into pGAD·C2) paired with pGBT9 empty vector. The bottom panel shows the *FOB1* derivatives paired with full-length *APC5* cloned into pGBT9. The cells were grown on SD −trp −leu to select for plasmids and on SD −trp −leu −ade to select for interactions. The positive control plasmids encode the SV40 large T-antigen (pTD1) and p53 (pVD3).

and the modified D box (**LXEXXXN**), referred to as the L box (Burton *et al.* 2005). The region flanking the E_{420} amino acid, corresponding to 1258–1263 bp is similar to the L box; $_{417}$**L**AN**E**AD**N**$_{423}$ (Figure 6A). To test whether the E_{420} amino acid is important for Fob1/Apc5 interactions, we created the E_{420}V mutation in C-terminal-tagged versions of *FOB1*. Destruction and KEN boxes are conserved and it often takes mutation to more than one motif to stabilize the APC substrate (Park *et al.* 2008). Therefore, we searched for additional potential APC interaction motifs within *FOB1* and identified D box 1, $_{306}$YGL**R**IG**L**G$_{313}$ (DB1), and D box 2, $_{542}$SKL**R**QK**L**D$_{549}$ (DB2). We altered these motifs by mutating the **R** and **L** amino acids within the motifs to **A** (Figure 6A).

To readily visualize modified forms of Fob1, we utilized a strain lacking *RPN10*, which encodes the proteasome ubiquitin receptor (Isasa *et al.* 2010). In the absence of Rpn10, we previously demonstrated that potential APC substrates accumulate within cells (Islam *et al.* 2011). Consistent with Fob1 modification, and perhaps ubiquitination, we observed an accumulation of higher molecular weight bands when we expressed Fob1-HA from the *GAL*-inducible promoter in asynchronous *rpn10*Δ cells (Figure 6B). This image was overexposed to observe higher molecular weight species of Fob1. Next, we expressed Fob1-HA mutant vectors DB1, DB2, DB1/DB2, and E420V in *rpn10*Δ cells and found a similar accumulation of higher molecular weight bands in all but the Fob1^{E420V}-HA construct (Figure 6C). The DB mutants followed the same expression patterns as WT Fob1-HA in WT and *rpn10*Δ cells; the DB mutants were low in WT cells, but accumulated in *rpn10*Δ cells. On the other hand, the E420V mutant was elevated in WT cells and remained unaltered in *rpn10*Δ cells. Interestingly, expression of Fob1^{E420V}-HA was similar in WT and *rpn10*Δ cells. These data suggest that Fob1 is modified post-translationally and that this modification requires glutamate at position 420.

Fob1 is an unstable protein that requires the APC and the L box for turnover

Our results suggest that the generation of slower migrating Fob1 bands in *rpn10*Δ cells requires an intact L box motif. Given Fob1's two-hybrid interaction with Apc5, we sought to determine whether Fob1 is targeted for degradation in an APC-dependent manner. We performed protein stability assays, as described above (Figure 4, B–D), to characterize Fob1 turnover in WT and *apc5^{CA}* cells expressing *GAL$_{pro}$-FOB1-HA* or *GAL$_{pro}$FOB1^{E420V}-HA*. The results showed that in WT cells, Fob1-HA was weakly detected after a 4-hr induction, with levels declining over the 2-hr release into CHX (Figure 7A). Fob1^{E420V}-HA accumulated to higher levels after 4 hr in galactose, with protein levels continuing to decrease

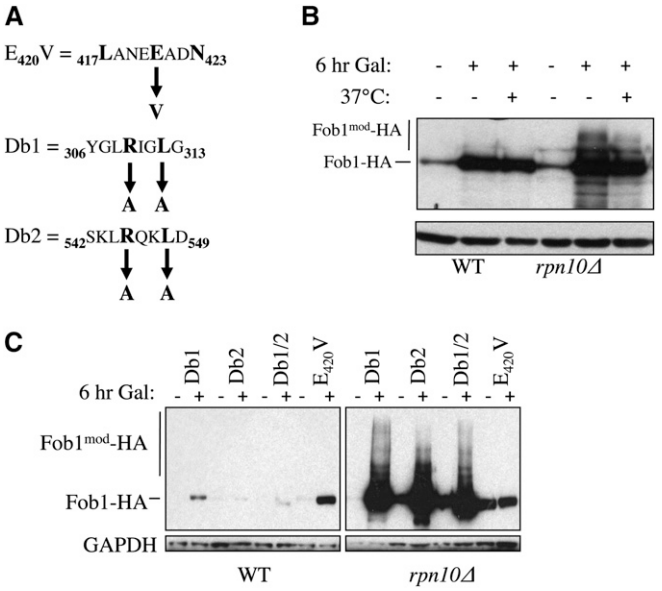

Figure 6 Fob1 modification requires the L box, a D box-like motif. (A) Creation of point mutations within *FOB1* that alter the putative APC interaction motifs: the L box, $E_{420}V$; DB1, $R_{309}A$, $L_{312}A$; and DB2, $R_{545}A$, $L_{548}A$. (B) Modified Fob1 bands ($Fob1^{mod}$) accumulate in *rpn10Δ* cells defective in proteosome polyubiquitin binding. WT and *rpn10Δ* cells expressing GAL_{pro}-*FOB1-HA* grown in glucose or galactose, at 30° or 37°C, to induce expression for 6 hr. (C) GAL_{pro}-*FOB1-HA* mutant plasmid constructs DB1, DB2, DB1DB2, and $E_{420}V$ in WT or *rpn10Δ* cells grown at 30° in glucose or galactose for 6 hr. Protein samples were analyzed by Westerns with antibodies against HA and GAPDH as a loading control.

after the 2-hr release. Comparison to WT cells indicated that Fob1 was indeed turned over and that the E420V mutation increased Fob1 accumulation, but did not completely block turnover. In $apc5^{CA}$ cells, Fob1-HA accumulated to yet higher levels after the 4-hr galactose induction and remained elevated throughout the 2-hr release. Similarly the $Fob1^{E420V}$ protein accumulated at equally high levels in $apc5^{CA}$ cells (Figure 7A). An analysis of Fob1 protein content showed that Fob1 turnover was slowed down in the E420V mutant, and slowed even further in $apc5^{CA}$ cells compared to WT (Figure 7B). Next, we compared total Fob1-HA levels after the 4-hr induction in galactose in WT and $apc5^{CA}$ cells expressing WT Fob1 or the $Fob1^{E420V}$ mutant (Figure 7C). $Fob1^{E420V}$ accumulated ~10-fold more than Fob1 in WT cells. In $apc5^{CA}$ cells, $Fob1^{E420V}$ accumulated ~15- to 17-fold more than the WT condition. Our results show that both intact Apc5 and the Fob1 E420 residue are required for efficient Fob1 turnover.

The $Fob1^{E420V}$ mutation increases rDNA recombination frequency

We predicted that a stable Fob1 protein should increase rDNA recombination. To discern whether the more stable $FOB1^{E420V}$ has any impact on rDNA recombination frequency, we introduced an endogenous $FOB1^{E420V}$ allele within the triple silencer recombination strain used above (Figure 3, C and D) and found that rDNA recombination did indeed increase in the $Fob1^{E420V}$ strain (Figure 8). This result reinforces our hypothesis that the insufficient removal of Fob1 by the defective $apc5^{CA}$ mutant leads to increased recombination and genomic instability within the rDNA region. Taken together, our results suggest a model whereby the APC at least in part regulates yeast mitotic lifespan and rDNA recombination through the targeted degradation of Fob1.

Discussion

Fob1, a potential novel APC binding partner

In a two-hybrid screen designed to discover novel APC binding partners that may serve as substrates, we identified a Fob1/Apc5 interaction. The Fob1/Apc5 interaction occurred in cells where the Apc5/GBT fusion protein was likely part of the intact APC, as this construct suppressed the $apc5^{CA}$ growth defect (data not shown). Therefore, Fob1 may not be interacting directly with Apc5, but instead with any APC subunit. Our preliminary coimmunoprecipitation experiments suggest at least that an Apc5-containing complex may physically interact with Fob1 (data not shown). Nonetheless, we identified a Fob1 domain with the potential capacity to facilitate APC interactions. The domain encompassed *FOB1* 1259–1263 bp, which encoded a motif that resembled a motif found in APC targets called the L box (Kim and Bonni 2007; Sullivan and Morgan 2007). The L box is similar in sequence to the Destruction (D) box. APC targets often harbor multiple D boxes and/or a KEN box, with mutation to one or more of these motifs capable of stabilizing APC targets (Burton *et al.* 2005). When overexpressed in strains lacking the *RPN10* proteasome ubiquitin receptor, Fob1 was observed to traverse through SDS–PAGE gels as a series of slowly migrating bands. This was abolished when a single residue within the L box was mutated ($Fob1^{E420V}$; Figure 6C). Furthermore, we demonstrated that Fob1 was unstable predominantly during G1, and that the E420V mutation stabilized the Fob1 protein (Figure 7A), which in turn, increased rDNA recombination frequency (Figure 8). Fob1 protein levels fluctuated throughout the cell cycle (Figure 4A), requiring an intact Apc5 (Figures 4B and 7A) and the G1-specific APC activator Cdh1 for turnover (Figure 4D). These observations support our notion that Fob1 is targeted for ubiquitination by the APC^{Cdh1} in G1. Despite this evidence, it remains possible that Fob1 is degraded in an APC-dependent manner, but itself is not a direct APC substrate. For instance, Fob1 may bind to an APC target protein, through the L box, which in turn stabilizes Fob1.

We also identified two additional motifs in Fob1 that resembled D box sequences, DB1 and DB2 (Figure 6A). Since mutation to DB1 and DB2 did not significantly contribute to Fob1 stabilization (data not shown) or abolish the slower migrating Fob1 species (Figure 6C), it is unlikely that either motif alone is required for APC interaction. However, since the L box mutation (E420V) did not completely abolish Fob1 turnover (Figure 7A), and weakly interacted with Apc5 in a two-hybrid experiment (Figure 5B), it remains possible that the DB motifs play a contributory role when combined with the L box.

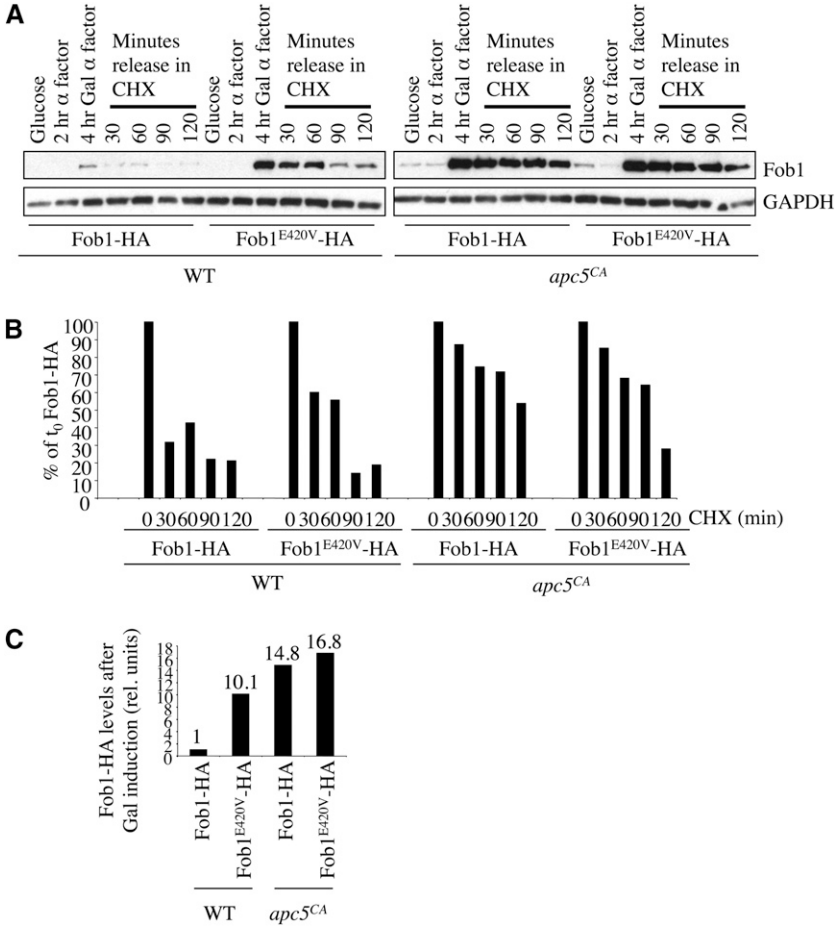

Figure 7 Fob1 is an unstable protein that requires the APC and the L box for turnover. (A) WT and *apc5*^{CA} cells expressing either *GAL*$_{pro}$*-FOB1-HA* or *GAL*$_{pro}$*-FOB1*^{E420V}*-HA* were arrested in G1 with α-factor, followed by induction of the *FOB1* constructs with galactose. Cells were then washed and released into fresh media containing CHX, with samples collected periodically for assessment of protein stability. Samples were analyzed by Westerns with antibodies against HA and GAPDH as a loading control. Films were scanned for analysis with ImageJ. (B) Band intensities from A were normalized to their corresponding GAPDH signal and then compared to band intensities after the 4-hr galactose induction. (C) The band intensity of WT Fob1 in WT cells after the 4-hr induction was set to 1. The band intensities from each sample after the 4-hr induction were compared to WT Fob1 in WT cells and plotted.

Reduction of Fob1 reduces rDNA recombination and genomic instability

The rDNA region is a considerable source of genomic instability due to its repetitive structure (Kobayashi 2011b; Vader *et al.* 2011). The short lived *apc5*^{CA} mutant has a broad range of genomic instability issues including chromatin assembly and histone metabolism defects (Harkness *et al.* 2002; 2005; Arnason *et al.* 2005; Turner *et al.* 2010; Islam *et al.* 2011), increased rDNA recombination (Figure 3D), and increased plasmid loss (Figure 3E; Harkness *et al.* 2002), which is an approximation of chromosome loss.

One function of Fob1 is to block and stall oncoming DNA replication forks within the rDNA region. The stalled replication machinery can result in DSBs and promote recombination (Kobayashi and Horiuchi 1996; Kobayashi *et al.* 1998). Homologous DNA repair of these DSBs can result in USCE due to the repeating structure of the rDNA. USCEs can result in duplication or deletion of one or more rDNA tandem repeats (Kobayashi *et al.* 1998; Ide *et al.* 2010). This process may be beneficial in an evolutionary sense, by maintaining a high copy number of rDNA repeats and insuring a high degree of homology among tandem repeats, but the increased frequency of stalled replication forks and DSBs within the rDNA region generates detrimental genomic instability in individual cells (Sinclair *et al.* 1997). It can be envisioned that the removal of Fob1 and the reduction of recombination would be beneficial to genomic stability, particularly in APC mutants, which are also impaired at resolving DSB breaks within the rDNA locus (Figure 3D). The deletion of *FOB1* significantly reduced rDNA recombination events and restored recombination frequency to WT levels in the *apc5*^{CA} background (Figure 3D). In contrast, the stabilized Fob1^{E420V} increased rDNA recombination (Figure 8). However, the deletion of *FOB1* did not cause global genomic instability, rather its effect appears to be exclusively localized to rDNA recombination (compare Figure 3, D and E). The *apc5*^{CA} mutation, on the other hand, affected global genomic stability, as plasmid loss in *apc5*^{CA} cells was increased (Figure 3E; Harkness *et al.* 2002). Furthermore, deletion of *FOB1* did not fully restore RLS to WT levels in *apc5*^{CA} and *apc10*Δ mutants, indicating that genomic instability outside of the rDNA locus in APC mutants may also impact RLS. Our results expose one particular pathway in which the APC impinges on genomic stability: the reduction of Fob1 levels and in turn rDNA recombination.

Reduction of cohesin within the rDNA locus may alleviate apc5^{CA} *defects*

The APC's primary function is to promote a timely separation of sister chromatids during anaphase. Sister chromatids are held together by cohesin, a clamp-like protein, and held

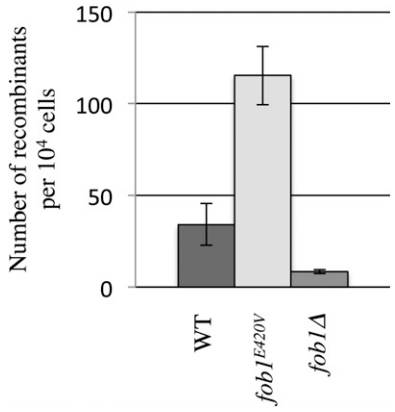

Figure 8 Fob1^{E420V} increases rDNA recombination frequency. The average frequency of rDNA recombination for five individual colonies of WT, *fob1*^{E420V}, and *fob1*Δ, as judged by the loss of the *ADE2* gene. Recombination frequency is expressed as the number of recombinant red colony forming units (CFUs) per 10^4 cells. Standard error of the mean is shown.

intact until all chromatids are attached to mitotic spindles (Remeseiro and Losada 2013). The removal of cohesin by separase is what allows the separation of sister chromatids. APC^{Cdc20} triggers the removal of cohesins by degrading securin, which in turn activates separase. The efficient rapid switch-like removal of cohesins is achieved by several positive feedback loops involving the simultaneous degradation of the cyclin component of cyclin-dependent kinases and release of the phosphatase Cdc14 from the nucleolus. The observation that *apc5*^{CA} cells accumulate in G2/M (Harkness *et al.* 2002; Arnason *et al.* 2005; Figure 3A) suggests that the robustness of this rapid switch-like removal of cohesins is compromised. This is likely due to delayed degradation of cyclins observed in *apc5*^{CA} cells (Figure 3B; Postnikoff *et al.* 2012), which in turn affects the synchrony of the positive feedback mechanisms. Degradation of other APC substrates, such as Clb5 and possibly Dbf4, aid in the required removal of rDNA-specific cohesin during chromosome segregation (Sullivan *et al.* 2008). Failure to remove rDNA-specific cohesins results in mitotic arrest or fatal unfaithful rDNA segregation (Johzuka and Horiuchi 2009).

A second important Fob1 function is to bind the RFB within the rDNA to recruit and anchor a variety of proteins within the nucleolus (Kobayashi and Horiuchi 1996; Kobayashi *et al.* 1998; Johzuka and Horiuchi 2002; Huang *et al.* 2006). Fob1 recruits the intra-S phase checkpoint components Tof2, Lrs4, and Csm1 to the rDNA locus (Huang *et al.* 2006). The interaction of Csm1 with cohesins (Newman *et al.* 2000; Graumann *et al.* 2004; Michaelis *et al.* 1997) suggests that Fob1 mediates the association of cohesins with rDNA. Lrs4 and Csm1 are released from the nucleolus during anaphase (Huang *et al.* 2006), which likely weakens the interaction between the rDNA and cohesins, providing an opportunity to segregate chromosomes. It is conceivable that the APC may be targeting Fob1 as early as anaphase to initiate release of Lrs4 and Csm1 from the nucleolus and aid in the segregation of the rDNA region during mitosis. Improved rDNA segregation during mitosis could contribute to improved RLS in the *FOB1* deletion.

The APC may play an important role in maintaining rDNA silencing through degradation of Fob1

Two recent studies have linked the APC with rDNA silencing and segregation (Sullivan *et al.* 2008; Dubey *et al.* 2009). Fob1 may be the target substrate for APC-dependent stability of the rDNA locus, as deletion of *FOB1* suppressed *apc5*^{CA} RLS, rDNA recombination, and cell cycle defects (Figure 1D and Figure 3, A, B, and D). However, Fob1 may play a role in maintaining genomic stability by recruiting the Sir2-containing RENT complex to rDNA while bound to the RFB site (Huang and Moazed 2003). This mechanism can facilitate silencing of rDNA intrachromatid recombination, which is in contrast to the DNA replication fork blocking function of Fob1 (Bairwa *et al.* 2010). In addition, Tof2, Lrs4, and Csm1 recruit condensins, proteins required for chromosome condensation, to the RFB site in a Fob1-dependent manner. Condensin recruitment to RFB sites is critical to facilitate higher order structure and rDNA integrity, conceivably by holding the tandem rDNA repeats in loops by an array of interacting condensins (Johzuka and Horiuchi 2009). This condensed, constrained Fob1-dependent structure may reduce rDNA recombination and transcription, which may be particularly important during nutrient starvation and quiescence (Tsang *et al.* 2007).

Conceivably, Fob1 dosage may be regulated by the APC as needed, to impinge upon rDNA silencing, in response to cell cycle and environmental cues (Figure 9). Our previous work supports the idea that the APC plays at least two roles in maintaining genomic stability. One is by ensuring proper chromatin metabolism upon exit from mitosis and entrance into G1 (Turner *et al.* 2010). The APC ensures histones are deposited onto DNA to form chromatin and then mediates proper histone modification to regulate transcription of genes needed to drive G1. Consistent with a role for the APC in rDNA stability, histone acetylation, specifically at K56 on histone H3, is involved in proper amplification of rDNA (Ide *et al.* 2013). Mutation to H3K56 or deletion of the genes that encode proteins involved in H3K56^{Ac}, such as *RTT109* or its binding partner *ASF1*, results in hyperamplification of rDNA. However, either increased or decreased H3K56^{Ac} caused rDNA hyperamplification, so the mechanism regulating rDNA amplification via H3K56^{Ac} remains unsolved. Interestingly, overexpression of *RTT109* or *ASF1*, as well as other genes that encode chromatin-modifying enzymes (*MSI1*, *CAC1*, *HIR1*, *HIR2*, *ELP3*, and *GCN5*), suppressed *apc5*^{CA} growth and/or chromatin assembly defects (Harkness *et al.* 2005; Turner *et al.* 2010). Thus, mutation to Apc5 may cause increased rDNA recombination through a mechanism involving Rtt109, Asf1, and H3K56^{Ac}.

A second APC function facilitating cell cycle progression is to target proteins for degradation once their job is complete during mitosis and G1. One such target is securin (Pds1). Targeted degradation of securin too early or too late will compromise accurate chromosomal segregation via cohesion

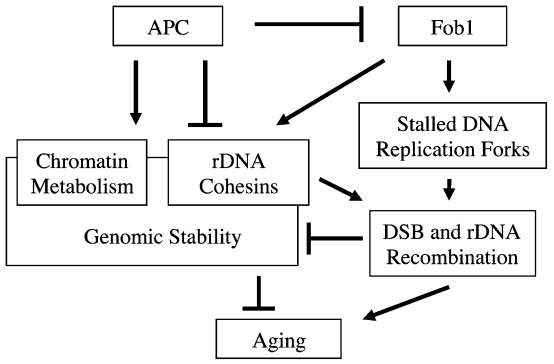

Figure 9 Model depicting how APC targeted degradation of Fob1 may regulate genomic stability and longevity. The APC impinges on genomic stability through a variety of mechanisms. Fob1 promotes genomic instability by increasing recruitment of cohesin to the rDNA, which when not removed, can result in incomplete sister chromatid segregation during mitosis, by stalling DNA replication machinery during S phase. Both of these mechanisms can result in DSBs and DNA recombination in this already highly unstable rDNA region.

removal, leading to genomic instability through events such as DSBs and rDNA recombination. Fob1 could also lead to genomic stability in two ways. First, Fob1 recruits the cohesins, and second, Fob1 stalls replication forks in the rDNA locus, leading to DSBs and rDNA recombination. The ability of the APC to target Fob1 for degradation at the proper time in the cell cycle may couple cell cycle progression and genomic stability with regulated longevity.

Acknowledgments

We thank Elizabeth Craig, Stan Fields, Takehiko Kobayashi, Walter Neupert, Kurt Runge, and Wei Xiao for strains and plasmids. Their generosity is greatly appreciated. Chelsea Stahl is thanked for her technical assistance. Mark Boyd is thanked for assistance with flow cytometry. This work was supported by grants to T.A.A.H. from the Canadian Foundation for Innovation and the Canadian Institutes for Health Research.

Literature Cited

Arnason, T. G., M. G. Pisclevich, M. D. Dash, G. F. Davies, and T. A. A. Harkness, 2005 Novel interaction between Apc5p and Rsp5p in an intracellular signaling pathway in *Saccharomyces cerevisiae*. Eukaryot. Cell 4: 134–146.

Ausubel, F. M., R. Brent, R. E. Kingston, D. D. Moore, J. G. Seidman *et al.*, 1995 *Current Protocols in Molecular Biology*, John Wiley & Sons, New York.

Bairwa, N. K., S. Zzaman, B. K. Mohanty, and D. Bastia, 2010 Replication fork arrest and rDNA silencing are two independent and separable functions of the replication terminator protein Fob1 of *Saccharomyces cerevisiae*. J. Biol. Chem. 285: 12612–12619.

Baker, D. J., K. B. Jeganathan, J. D. Cameron, M. Thompson, S. Juneja *et al.*, 2004 BubR1 insufficiency causes early onset of aging-associated phenotypes and infertility in mice. Nat. Genet. 36: 744–749.

Barford, D., 2011 Structural insights into anaphase-promoting complex function and mechanism. Philos. Trans. R. Soc. Lond. B Biol. Sci. 366: 3605–3624.

Burton, J. L., V. Tsakraklides, and M. J. Solomon, 2005 Assembly of an APC-Cdh1-substrate complex is stimulated by engagement of a destruction box. Mol. Cell 18: 533–542.

Chan, K. S., C. G. Koh, and H. Y. Li, 2012 Mitosis-targeted anticancer therapies: where they stand. Cell Death Dis. 18: 3:e411.

Dang, W., K. K. Steffen, R. Perry, J. A. Dorsey, F. B. Johnson *et al.*, 2009 Histone H4 lysine 16 acetylation regulates cellular life span. Nature 459: 802–807.

Defossez, P. A., R. Prusty, M. Kaeberlein, S. J. Lin, P. Ferrigno *et al.*, 1999 Elimination of replication block protein Fob1 extends the life span of yeast mother cells. Mol. Cell 3: 447–455.

Dubey, R. N., N. Nakwal, K. K. Bisht, A. Saini, S. Haldar *et al.*, 2009 Interaction of APC/C-E3 ligase with Swi6/HP1 and Clr4/Suv39 in heterochromatin assembly in fission yeast. J. Biol. Chem. 284: 7165–7176.

Ferguson, J. L., W. C. Chao, E. Lee, and K. L. Friedman, 2013 The anaphase promoting complex contributes to the degradation of the S. cerevisiae telomerase recruitment subunit Est1p. PLoS ONE 8: e55055.

Feser, J., D. Truong, C. Das, J. J. Carson, J. Kieft *et al.*, 2010 Elevated histone expression promotes life span extension. Mol. Cell 39: 724–735.

Ganley, A. R., S. Ide, K. Saka, and T. Kobayashi, 2009 The effect of replication initiation on gene amplification in the rDNA and its relationship to aging. Mol. Cell 35: 683–693.

Graumann, J., L. A. Dunipace, J. H. Seol, W. H. McDonald, J. R. Yates *et al.*, 2004 Applicability of tandem affinity purification MudPIT to pathway proteomics in yeast. Mol. Cell. Proteomics 3: 226–237.

Greer, E. L., T. J. Maures, D. Ucar, A. G. Hauswirth, E. Mancini *et al.*, 2011 Transgenerational epigenetic inheritance of longevity in *Caenorhabditis elegans*. Nature 479: 365–371.

Han, S., and A. Brunet, 2012 Histone methylation makes its mark on longevity. Trends Cell Biol. 22: 42–49.

Harkness, T. A. A., 2005 Chromatin assembly from yeast to man: Conserved factors and conserved molecular mechanisms. Curr. Genomics 6: 227–240.

Harkness, T. A. A., 2006 The anaphase promoting complex and aging: The APCs of longevity. Curr. Genomics 7: 263–272.

Harkness, T. A. A., G. F. Davies, V. Ramaswamy, and T. G. Arnason, 2002 The ubiquitin-dependent targeting pathway in *Saccharomyces cerevisiae* plays a critical role in multiple chromatin assembly regulatory steps. Genetics 162: 615–632.

Harkness, T. A. A., K. A. Shea, C. Legrand, M. Brahmania, and G. F. Davies, 2004 A functional analysis reveals dependence on the anaphase-promoting complex for prolonged life span in yeast. Genetics 168: 759–774.

Harkness, T. A. A., T. G. Arnason, C. Legrand, M. G. Pisclevich, G. F. Davies *et al.*, 2005 Contribution of CAF-I to anaphase-promoting-complex-mediated mitotic chromatin assembly in *Saccharomyces cerevisiae*. Eukaryot. Cell 4: 673–684.

Harper, J. W., J. L. Burton, and M. J. Solomon, 2002 The anaphase-promoting complex: it's not just for mitosis any more. Genes Dev. 16: 2179–2206.

Hartwell, L. H., and D. Smith, 1985 Altered fidelity of mitotic chromosome transmission in cell cycle mutants of *S. cerevisiae*. Genetics 110: 381–395.

Huang, J., and D. Moazed, 2003 Association of the RENT complex with nontranscribed and coding regions of rDNA and a regional requirement for the replication fork block protein Fob1 in rDNA silencing. Genes Dev. 17: 2162–2176.

Huang, J., I. L. Brito, J. Villén, S. P. Gygi, A. Amon *et al.*, 2006 Inhibition of homologous recombination by a cohesin-

associated clamp complex recruited to the rDNA recombination enhancer. Genes Dev. 20: 2887–2901.
Ide, S., T. Miyazaki, H. Maki, and T. Kobayashi, 2010 Abundance of ribosomal RNA gene copies maintains genome integrity. Science 327: 693–696.
Ide, S., K. Saka, and T. Kobayashi, 2013 Rtt109 prevents hyperamplification of ribosomal RNA genes through histone modification in budding yeast. PLoS Genet. 9: e1003410.
Isasa, M., E. J. Katz, W. Kim, V. Yugo, S. González *et al.*, 2010 Monoubiquitination of RPN10 regulates substrate recruitment to the proteasome. Mol. Cell 38: 733–745.
Islam, A., E. L. Turner, J. Menzel, M. E. Malo, and T. A. A. Harkness, 2011 Antagonistic Gcn5-Hda1 interactions revealed by mutations to the Anaphase Promoting Complex in yeast. Cell Div. 6: 13.
Ito, K., T. Sugawara, M. Shiroishi, N. Tokuda, A. Kurokawa *et al.*, 2008 Advanced method for high-throughput expression of mutated eukaryotic membrane proteins in *Saccharomyces cerevisiae*. Biochem. Biophys. Res. Commun. 371: 841–845.
James, P., J. Halladay, and E. A. Craig, 1996 Genomic libraries and a host strain designed for highly efficient two-hybrid selection in yeast. Genetics 144: 1425–1436.
Johzuka, K., and T. Horiuchi, 2002 Replication fork block protein, Fob1, acts as an rDNA region specific recombinator in *S. cerevisiae*. Genes Cells 7: 99–113.
Johzuka, K., and T. Horiuchi, 2009 The cis element and factors required for condensin recruitment to chromosomes. Mol. Cell 34: 26–35.
Kennedy, B. K., N. R. Austriaco, Jr., and L. Guarente, 1994 Daughter cells of Saccharomyces cerevisiae from old mothers display a reduced life span. J. Cell Biol. 127: 1985–1993.
Kim, A. H., and A. Bonni, 2007 Thinking within the D box: initial identification of Cdh1-APC substrates in the nervous system. Mol. Cell. Neurosci. 34: 281–287.
Ko, N., R. Nishihama, G. H. Tully, D. Ostapenko, M. J. Solomon *et al.*, 2007 Identification of yeast IQGAP (Iqg1p) as an anaphase-promoting-complex substrate and its role in actomyosin-ring-independent cytokinesis. Mol. Biol. Cell 18: 5139–5153.
Kobayashi, T., 2011a How does genome instability affect lifespan?: roles of rDNA and telomeres. Genes Cells 16: 617–624.
Kobayashi, T., 2011b Regulation of ribosomal RNA gene copy number and its role in modulating genome integrity and evolutionary adaptability in yeast. Cell. Mol. Life Sci. 68: 1395–1403.
Kobayashi, T., and A. R. Ganley, 2005 Recombination regulation by transcription-induced cohesin dissociation in rDNA repeats. Science 309: 1581–1584.
Kobayashi, T., and T. Horiuchi, 1996 A yeast gene product, Fob1 protein, required for both replication fork blocking and recombinational hotspot activities. Genes Cells 1: 465–474.
Kobayashi, T., D. J. Heck, M. Nomura, and T. Horiuchi, 1998 Expansion and contraction of ribosomal DNA repeats in Saccharomyces cerevisiae: requirement of replication fork blocking (Fob1) protein and the role of RNA polymerase I. Genes Dev. 12: 3821–3830.
Lewy, G. D., N. Sharma, R. I. Seed, V. E. Smith, K. Boelaert *et al.*, 2012 The pituitary tumor transforming gene in thyroid cancer. J. Endocrinol. Invest. 35: 425–433.
Marinus, M. G., and N. R. Morris, 1975 Pleiotropic effects of a DNA adenine methylation mutation (dam-3) in Escherichia coli K12. Mutat. Res. 28: 15–26.
McLean, J. R., D. Chaix, M. D. Ohi, and K. L. Gould, 2011 State of the APC/C: organization, function, and structure. Crit. Rev. Biochem. Mol. Biol. 46: 118–136.
McMurray, M. A., and D. E. Gottschling, 2004 Aging and genetic instability in yeast. Curr. Opin. Microbiol. 7: 673–679.
Michaelis, C., R. Ciosk, and K. Nasmyth, 1997 Cohesins: chromosomal proteins that prevent premature separation of sister chromatids. Cell 91: 35–45.
Mohanty, B. K., and D. Bastia, 2004 Binding of the replication terminator protein Fob1p to the Ter sites of yeast causes polar fork arrest. J. Biol. Chem. 279: 1932–1941.
Mohanty, B. K., N. K. Bairwa, and D. Bastia, 2009 Contrasting roles of checkpoint proteins as recombination modulators at Fob1-Ter complexes with or without fork arrest. Eukaryot. Cell 8: 487–495.
Newman, J. R., E. Wolf, and P. S. Kim, 2000 A computationally directed screen identifying interacting coiled coils from Saccharomyces cerevisiae. Proc. Natl. Acad. Sci. USA 97: 13203–13208.
Ostapenko, D., J. L. Burton, and M. J. Solomon, 2012 Identification of anaphase promoting complex substrates in *S. cerevisiae*. PLoS ONE 7: e45895.
Palmer, R. E., E. Hogan, and D. Koshland, 1990 Mitotic transmission of artificial chromosomes in cdc mutants of the yeast, *Saccharomyces cerevisiae*. Genetics 125: 763–774.
Pan, Y., 2011 Mitochondria, reactive oxygen species, and chronological aging: a message from yeast. Exp. Gerontol. 46: 847–852.
Park, H. J., R. H. Costa, L. F. Lau, A. L. Tyner, and P. Raychaudhuri, 2008 Anaphase-promoting complex/cyclosome-CDH1-mediated proteolysis of the forkhead box M1 transcription factor is critical for regulated entry into S phase. Mol. Cell. Biol. 28: 5162–5171.
Passmore, L. A., 2004 The anaphase-promoting complex (APC): The sum of its parts? Biochem. Soc. Trans. 32(Pt 5): 724–727.
Postnikoff, S. D., M. E. Malo, B. Wong, and T. A. A. Harkness, 2012 The yeast Forkhead transcription factors Fkh1 and Fkh2 regulate lifespan and stress response together with the Anaphase Promoting Complex. PLoS Genet. 8: e1002583.
Qiao, X., L. Zhang, A. M. Gamper, T. Fujita, and Y. Wan, 2010 APC/C-Cdh1: from cell cycle to cellular differentiation and genomic integrity. Cell Cycle 9: 3904–3912.
Remeseiro, S., and A. Losada, 2013 Cohesin, a chromatin engagement ring. Curr. Opin. Cell Biol. 25: 63–71.
Riesen, M., and A. Morgan, 2009 Calorie restriction reduces rDNA recombination independently of rDNA silencing. Aging Cell 8: 624–632.
Rodríguez-Sánchez, L., M. Rodríguez-López, Z. García, M. Tenorio-Gómez, J. B. Schvartzman *et al.*, 2011 The fission yeast rDNA-binding protein Reb1 regulates G1 phase under nutritional stress. J. Cell Sci. 124: 25–34.
Roy, N., and K. W. Runge, 2000 Two paralogs involved in transcriptional silencing that antagonistically control yeast life span. Curr. Biol. 10: 111–114.
Seviour, E. G., and S. Y. Lin, 2010 The DNA damage response: balancing the scale between cancer and ageing. Aging 2: 900–907.
Sinclair, D. A., and L. Guarente, 1997 Extrachromosomal rDNA circles: a cause of aging in yeast. Cell 91: 1033–1042.
Sinclair, D. A., K. Mills, and L. Guarente, 1997 Accelerated aging and nucleolar fragmentation in yeast sgs1 mutants. Science 277: 1313–1316.
Smith, V. E., J. A. Franklyn, and C. J. McCabe, 2010 Pituitary tumor-transforming gene and its binding factor in endocrine cancer. Expert Rev. Mol. Med. 12: e38.
Smolders, L., and J. G. Teodoro, 2011 Targeting the anaphase promoting complex: common pathways for viral infection and cancer therapy. Expert Opin. Ther. Targets 15: 767–780.
Straight, A. F., W. Shou, G. J. Dowd, C. W. Turck, R. J. Deshaies *et al.*, 1999 Net1, a Sir2-associated nucleolar protein required for rDNA silencing and nucleolar integrity. Cell 97: 245–256.
Sullivan, M., and D. O. Morgan, 2007 A novel destruction sequence targets the meiotic regulator Spo13 for anaphase-promoting complex-dependent degradation in anaphase I. J. Biol. Chem. 282: 19710–19715.

Sullivan, M., L. Holt, and D. O. Morgan, 2008 Cyclin-specific control of ribosomal DNA segregation. Mol. Cell. Biol. 28: 5328–5336.

Tsang, C. K., H. Li, and X. S. Zheng, 2007 Nutrient starvation promotes condensin loading to maintain rDNA stability. EBMO J. 26: 448–458.

Turner, E. L., M. E. Malo, M. G. Pisclevich, M. D. Dash, G. F. Davies *et al.*, 2010 The *Saccharomyces cerevisiae* anaphase-promoting complex interacts with multiple histone-modifying enzymes to regulate cell cycle progression. Eukaryot. Cell 9: 1418–1431.

Vader, G., H. G. Blitzblau, M. A. Tame, J. E. Falk, and L. Curtin, L. *et al.*, 2011 Protection of repetitive DNA borders from self-induced meiotic instability. Nature 477: 115–119.

Wang, Z., L. Wan, J. Zhong, H. Inuzuka, and P. Liu *et al.*, 2013 Cdc20: a potential novel therapeutic target for cancer treatment. Curr. Pharm. Des. 19: 3210–3214.

Wäsch, R., J. A. Robbins, and F. R. Cross, 2010 The emerging role of APC/CCdh1 in controlling differentiation, genomic stability and tumor suppression. Oncogene 29: 1–10.

Wei, Z., S. Peddibhotla, H. Lin, X. Fang, M. Li *et al.*, 2011 Early-onset aging and defective DNA damage response in Cdc14b-deficient mice. Mol. Cell. Biol. 31: 1470–1477.

Zachariae, W., and K. Nasmyth, 1999 Whose end is destruction: cell division and the anaphase-promoting complex. Genes Dev. 13: 2039–2058.

Zhu, G., P. T. Spellman, T. Volpe, P.O. Brown, D. Botstein *et al.*, 2000 Two yeast forkhead genes regulate the cell cycle and pseudohyphal growth. Nature 406: 90–94.

Zuin, A., D. Castellano-Esteve, J. Ayté, and E. Hidalgo, 2010 Living on the edge: stress and activation of stress responses promote lifespan extension. Aging 2: 231–237.

Communicating editor: O. Cohen-Fix